Structures and Electronic Properties of the Small Rubidium-Doped Silicon RbSin (n=1-12) Clusters

ARTICLE *in* INTERNATIONAL JOURNAL OF QUANTUM CHEMISTRY · JANUARY 2015

Impact Factor: 1.43 · DOI: 10.1002/qua.24796

6 AUTHORS, INCLUDING:

Chaozheng He

Nanyang Normal University

37 PUBLICATIONS **85** CITATIONS

SEE PROFILE

Zhang Shuai

Nanyang Normal University

19 PUBLICATIONS **18** CITATIONS

SEE PROFILE

International Journal of QUANTUM CHEMISTRY

Structures and Electronic Properties of the Small Rubidium-Doped Silicon $RbSi_n$ ($n = 1–12$) Clusters

Chang-Geng Luo, Chao-Zheng He, Hua-Yang Li, Gen-Quan Li, Shuai Zhang,* and Xu-Yan Liu

The geometries, relative stabilities, and electronic properties of small rubidium-doped silicon clusters $RbSi_n$ ($n = 1–12$) have been systematically investigated using the density functional theory at the B3LYP/GENECP level. The optimized structures show that lowest-energy isomers of $RbSi_n$ are similar with the ground state isomers of pure Si_n clusters and prefer the three-dimensional for $n = 3–12$. The relative stabilities of $RbSi_n$ clusters have been analyzed on the averaged binding energy, fragmentation energy, second-order energy difference, and highest occupied molecular orbital-lowest unoccupied molecular orbital energy gap. The calculated results indicate that the doping of Rb atom enhances the chemical activity of Si_n frame and the magic number is $RbSi_2$. The Mulliken population analysis reveals that the charges in the corresponding $RbSi_n$ clusters transfer from the Rb atom to Si atoms. The partial density of states and chemical hardness are also discussed. © 2014 Wiley Periodicals, Inc.

DOI: 10.1002/qua.24796

Introduction

In the past few decades, the clusters composed of metals and silicon have attracted considerable attentions due to their specific chemical and physical properties as well as their applications in the construction of microelectronic devise.[1–6] Specially, the studies of alkali metal silicon clusters are of significant importance because the new materials obtained from the reaction of alkali metal atoms with semiconductor surfaces, which have been widely used in many products, such as promoters in catalysts, emitters, spaceflight aerocrafts, and so forth.[7–9] Many alkali metal-doped silicon clusters have been studied in great detail by numerous experimental[10–12] and theoretical works.[13–15] Based on the technique of laser vaporization, Kishi et al.[10] carried out an experiment to produce the Si—Na binary clusters (Si_nNa_m). In addition, they also determined the ionization energies of Si_nNa_m clusters from the threshold energies of ionization efficiency curves using the commercial UV laser. Zubarev et al.[11] explored the structure and bonding in Si_6^{2-}, Si_6^{2-}, and $NaSi_6^-$ using photoelectron spectroscopy and pointed out that the spectra of $NaSi_6^-$ are similar to those of Si_6^-. Using the photoionization efficiency measurements and mass spectroscopy, Tam et al.[12] studied the geometric and electronic structures of neutral and cationic $Si_nLi_m^{0/+}$ clusters ($n = 2–11$, $m = 1$, 2) and revealed that the shape of the cationic isomers are similar with their corresponding neutral isomers. Theoretically, Sporea et al.[13] systematically investigated the structures, population analysis, and electric dipole moments of small mixed alkali-silicon clusters Si_nM_p (M = Li, Na, and K, $n = 1–6$, $p = 1$, 2) using the density functional theory (DFT). The results showed that the ground state structures of Si_nM_p keep the frame of the corresponding Si_n clusters unchanged and the alkali atoms being adsorbed at the surface. Subsequently, Sporea and Rabilloud[14] calculated the structure, stability, and electronic properties of the alkali metal-doped Si clusters $A@Si_n$ (A = Li, Na, and K, $n = 10–20$). They found that the charge always transfers from the alkali metal atom to the Si atoms and the larger clusters prefer to retain the alkali atom as the encapsulated atom in $A@Si_n$ cage clusters. Based on the Møller–Plesset perturbation (MP2) and coupled cluster theory, Karamanis et al.[15] investigated and discussed the polarizabilities of alkali (Li, Na, and K)-doped Si_{10} by means of *ab initio* methods. The results indicated that while alkali doping leaves the per atom polarizability practically unaffected, influences dramatically the hyperpolarizabilities of Si_{10}. Recently, Blair and Thakkar[16] explored the semiquantitative relationships between the mean static dipole polarizability and other molecular properties, for example, the electronegativity, ionization energy, hardness, volume, and moments of momentum.

Rubidium is a very reactive alkali metal element with complex electronic configuration $4s^24p^65s^1$, which has high positive electricity and maximum photoelectric effects. It has been widely used in many fields, such as: phototube, catalyst, vacuum tube, photocells, and cathode ray tube. The rubidium-silicon system has been extensively studied[17–20] because the new materials synthesized by the reaction of Rb with Si can be widely used, such as electronic devices, catalysts, special glass, thermionic conversion power, and biochemistry.

C.-G. Luo, C.-Z. He, H.-Y. Li, G.-Q. Li, S. Zhang and X.-Y. Liu
Department of Physics, Nanyang Normal University, Nanyang, 473061, China
E-mail: nynuzhang@163.com

Contract grant sponsor: Natural Science Foundation of China.
Contract grant sponsor: 11304167, 61306007.
Contract grant sponsor: Postdoctoral Science Foundation of China.
Contract grant sponsor: 20110491317.
Contract grant sponsor: Natural Science Foundation of Nanyang Normal University; contract grant number: 132300410209.

Table 1. Calculated and experimental bond lengths (r), vertical ionization potential (VIP), and frequencies (ω) of RhSi, Rh_2, and Si_2 clusters.

	RbSi			Rb_2			Si_2		
Methods	r (Å)	ω (cm^{-1})	VIP (eV)	r (Å)	ω (cm^{-1})	VIP (eV)	r (Å)	ω (cm^{-1})	VIP (eV)
PW91	3.36	143.58	5.39	4.25	53.77	4.09	2.30	468.72	8.27
PBE	3.37	142.99	5.56	4.26	53.46	3.88	2.30	468.76	8.23
BP86	3.38	140.93	5.59	4.23	54.03	4.15	2.30	465.6	8.32
B3LYP	3.39	141.36	5.38	4.24	54.4	4.07	2.28	485.5	8.60
Experiment	–	–	–		57.31[39]	3.9 ± 0.1[40]	2.25[41]	511.0[41]	>8.49[42]

Although enormous progress that has been made, little is known about the geometric structure and electronic properties of Rb-doped Si_n clusters, and the physical origin of its electronic properties is still not well understood. There are many problems about the $RbSi_n$ clusters need to be studied. These issues include: (i) What are the growing patterns of $RbSi_n$ clusters? (ii) Can Rb atom in $RbSi_n$ clusters completely falls into the interior of Si frame and forms metal-encapsulated Si cage at a certain size? (iii) What are the charge transfer mechanisms of the $RbSi_n$ clusters? So, it is necessary to probe the influence of impurity Rb atom on the structures and electronic properties of the $RbSi_n$ clusters. In this work, we performed a theoretical study on the $RbSi_n$ ($n = 1$–12) clusters and compared with that of the pure Si_{n+1} clusters. Our main objective is to gain a fundamental understanding of the most stable structures in $RbSi_n$ clusters and to provide a significant understanding for further theoretical and experimental studies.

Computational Details

All the geometrical and electronic structures of the $RbSi_n$ clusters have been performed using DFT as implemented in the Gaussian 09 package.[21] The B3LYP exchange-correlation potential, which uses Becke's three-parameter functional with the Lee-Yang-Parr correlation functional, is used.[22,23] Because the Rb is a heavy atom, the full electron calculations are rather time-consuming, so the effective core potential (ECP) including relativistic effects are considered. The 6-311+G(d) basis set, which is triple ζ and has the d polarization functions, is used for all the Si atoms. Thus, the basis set labeled GENECP (LANL2DZ for the Rb atom and 6-311+G(d) for the Si atoms) is adopted. The application of the B3LYP/GENECP method has been shown to be effective for many small-sized heteroatom-doped silicon clusters.[24–27] To obtain the global minimum, a great deal of initial geometries, which include one-, two-, and three-dimensional (3D) configurations, are studied in the following ways: (1) on the basis of many previous studies Si_n and XSi_n structures,[28–38] we optimized the geometries of pure Si_n clusters; (2) the initial structures of $RbSi_n$ clusters are obtained by placing Rb atom at various places of the optimized Si_n geometries, that is, Rb-capped, Rb-substituted, and Rb-encapsulated patterns. For all isomers, the harmonic vibration frequencies are computed to guarantee the optimized geometries corresponding to the global minimum without any imaginary mode.

To check the accuracy of our calculations, the bond length (r), vibrational frequency (ω), and vertical ionization potential (VIP) of Si_2, Rb_2, and RbSi dimers are calculated using different functionals. The calculated results as well as the experimental data are summarized in the Table 1. From the table, it is obviously that the results based on the B3LYP method are in good agreement with the experimental values[39–42] than the others. So, the calculation method in this work is suitable and accurate enough.

Results and Discussions

Structures of $RbSi_n$ ($n = 1$–12) clusters

Using the computational method described in Computational Details Section, we have studied many possible initial configurations and gained the ground state structures for $RbSi_n$ ($n = 1$–12) clusters. Figure 1 illustrates the most stable and some selected low-lying isomers. These isomers are denoted by their energy orders from low to high as *n*a, *n*b, *n*c, *n*d, and *n*e ("*n*" is the number of Si atoms in $RbSi_n$ clusters), with *n*a being the lowest-energy isomer. Meanwhile, in order to compare the effects of dopant Rb atom on silicon clusters, we have carried out some geometry optimizations of Si_{n+1} clusters using the same method and basis set. The ground state structures of Si_{n+1} clusters are also plotted in Figure 1.

For RbSi, the calculated results show that the doublet and sextet spin states are much higher in energy than the quartet spin states by 0.32 and 5.61 eV, respectively. Hence, the quartet spin ($^4\sum$) RhSi dimer is the most stable structure. This feature is similar with previous TMSi (TM = Ta, Sc, Y, and Re),[38,43–45] which have the ground state structures with a quartet spin configuration. The Rb—Si bond length is 3.39 Å, which is shorter than the Rh—Rh bond length (4.24 Å) and longer than the bond distance of Si_2 isomer (2.28 Å). This fact perhaps caused by the reason that much weaker relativistic effects in the RbSi cluster exist than that in the Si_2 cluster. For $n = 2$, possible configurations such as triangular and linear isomers are considered. The calculated results show that the most stable isomer (2a) is an isosceles triangular structure with C_{2v} symmetry. This structure is similar to previous most stable structure of XSi_2 (X = Li, Na, K, Sc, and Y).[33–35,43,44] The linear chain Si—Rb—Si (2b in Fig. 1) isomer is higher in energy than that of 2a by 3.28 eV. For $RbSi_3$, our calculated data indicate that the triple prism structure 3a with one Rb atom occupying the vertex is the most stable isomer. This finding is very similar to those of the $TaSi_3$, VSi_3^- and WSi_3[38,46,47] clusters. The previous studies reported that the planar rhombus structure is

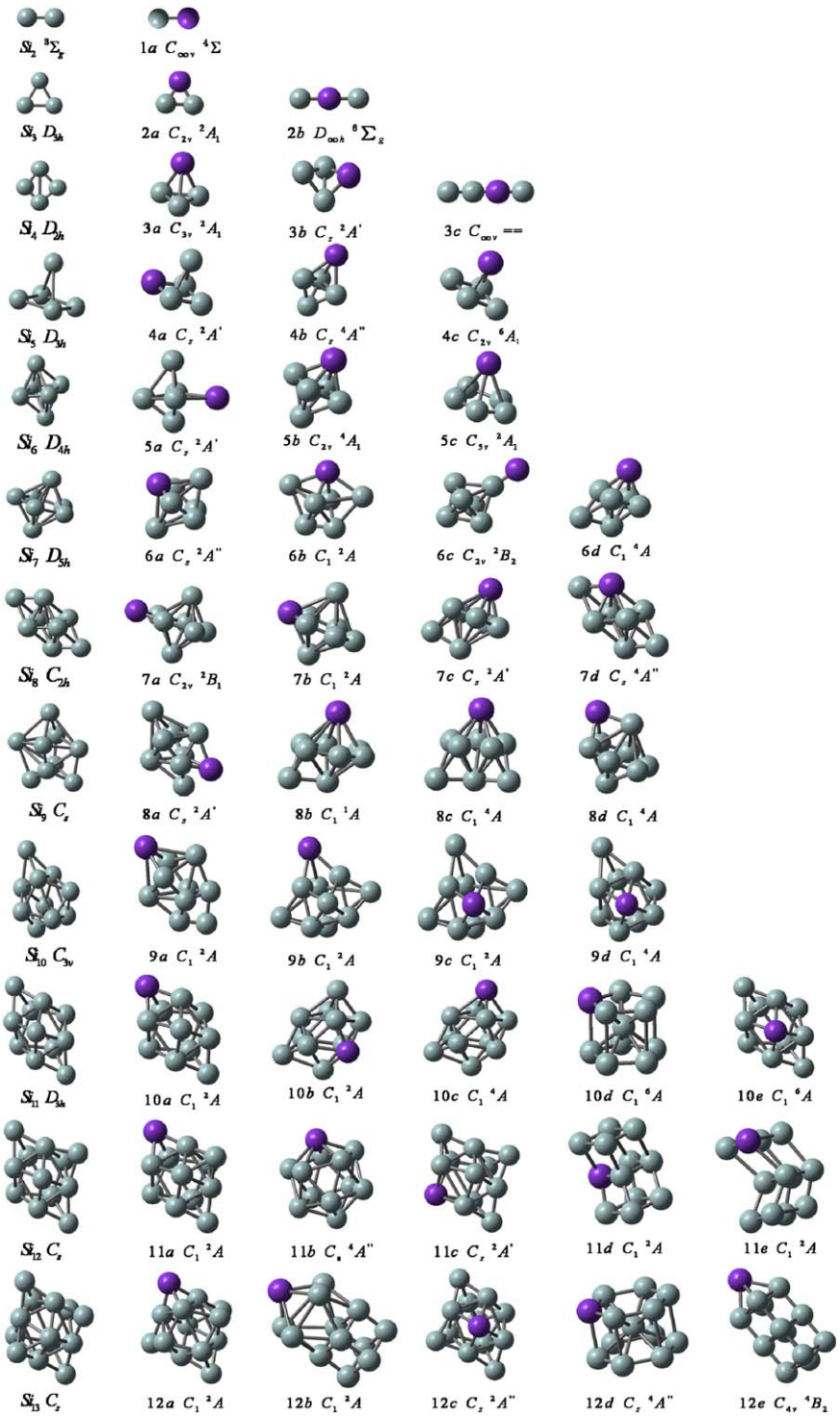

Figure 1. The lowest-energy structures of Si_{n+1} and $RbSi_n$ ($n = 1$–12), and a few low-lying isomers for doped clusters. Gray and purple balls represent Si and Rb atoms, respectively.

the global minimum for $LiSi_3$, $NaSi_3$, KSi_3, $ScSi_3$, and YSi_3[33–35,43,44] clusters. However, this structure does not exist in $RbSi_n$ clusters. This indicates that the different dopant atoms have significant effect on the silicon clusters. The isomer 3b (C_s) is a butterfly structure with 0.14 eV higher in energy than that of 3a isomer. The two-dimensional isomer 3c ($C_{\infty V}$) is a linear structure with Rb atom in the middle. It is 0.25 eV higher than 3a isomer. Compared with the corresponding Si_4 cluster, the most stable $RbSi_3$ cluster (4a) can be regarded as a substituted structure of the pure silicon cluster. The trigonal bipyramid isomer 4b shows a similar structure to the ground state of $TMSi_4$ (M = Lu and Zr),[48,49] which is less stable than 4a isomer by 0.46 eV. The isomer 4c is similar to the geometry of isomer 4a. However, they have different electronic states and symmetries

Table 2. The averaged binding energy $E_b(n)$, fragmentation energy $E_f(n)$, second-order energy difference $\Delta_2E(n)$, HOMO-LUMO energy gaps E_{gap}, the lowest and highest vibration frequency, atomic charges, and density of states (DOS) of s, p orbital at the vicinity of Fermi level of $RbSi_n$ ($n = 1$–12) clusters.

					Frequency (cm^{-1})					
	E_b (eV)	E_f (eV)	Δ_2E (eV)	E_{gap} (eV)	Lowest	Highest	Charge (e)	ρ_p $(eV)^{-1}$	ρ_s $(eV)^{-1}$	ρ_n $(eV)^{-1}$
1	0.55	1.11		1.27		141.36	0.662	1.5000	0.175	1.675
2	1.61	3.72	1.40	1.62	91.90	574.51	0.707	0.315	0.110	0.425
3	1.78	2.31	−2.40	0.52	18.50	463.92	0.813	1.500	0.475	1.975
4	2.37	4.73	0.72	1.59	32.68	457.84	0.846	3.500	0.375	3.875
5	2.64	3.53	0.47	1.95	15.59	451.56	0.881	0.210	0.062	0.272
6	2.77	4.01	0.64	1.76	38.32	427.86	0.872	0.153	0.008	0.161
7	2.83	3.28	0.25	1.56	23.14	400.42	0.840	3.500	0.498	3.998
8	2.81	2.64	−1.07	1.40	29.05	475.60	0.819	3.602	1.200	4.802
9	2.90	3.71	−0.32	1.39	17.83	521.53	0.855	1.800	0.200	2.000
10	3.00	4.03	1.39	1.23	37.52	440.85	0.795	2.380	0.201	2.581
11	2.97	2.63	−0.39	1.31	26.35	461.35	0.786	0.081	0.022	0.103
12	2.98	3.02		1.21	34.06	473.72	0.803	2.190	0.402	2.592

and the former is 0.87 eV higher in total energy than the latter. Among $RbSi_5$ clusters, the isomer 5a with C_s symmetry and $^2A'$ electronic state, which originated from the metastable isomer Si_6[28] by replacing one Si atom with one Rb atom, is the lowest-energy structure. The isomer 5b is a substituted geometry of Si_6, in which one Rb atom replaces one Si atom of tetragonal bipyramid structure. Its energy is 0.89 eV higher than 5a isomer. The isomer 5c is a pentagonal pyramid structure, which is 1.53 eV higher than that of ground state 5a. Similar to the geometry of the lowest-energy Si_7 cluster, the pentagonal bipyramid 6a isomer with Rb atom on the base is the ground state structure of $RbSi_6$ clusters. The similar location preferences (base atom location) are also found for the most stable geometries of NSi_6,[50] PSi_6,[51] and $MnSi_6^+$[52] clusters. After one Si is capped on the 5a geometry, the boat-like isomer 6b is generated. When the 5b isomer is capped with one Rb or Si atom, the less stable isomers 6c and 6d are obtained. The total energy of 6b, 6c, and 6d are 0.09, 0.37, and 1.37 eV higher than that of 6a isomer, respectively.

When $n = 7$, the lowest-energy isomer 7a with C_{2v} symmetry is generated by capping the Si_7 cluster with one Rb atom, which resembles the most stable structure of $MnSi_7^+$[52] cluster. The isomer 7b is a double hexagonal pyramid with Rb atom on the base and is 0.12 eV higher in energy than 7a isomer. When one Rb atom is capped on the 6a structure, isomer 7c is generated. The least stable isomer 7d can be obtained by capping one Si atom on the 6d structure. The isomers 7c and 7d are above the ground state by 0.65 and 0.89 eV, respectively. For $RbSi_8$, the most stable isomer 8a can be viewed as a substituted version of the structure of the ground state Si_9 cluster. The isomer 8b with Rb atom on the vertex is different in energy from the similar structure 8d with Rb atom on one side. The isomer 8c, which is 0.76 eV higher in energy than 8a, can be obtained by capping one Si atom on the 7c. For $n = 9$, the lowest-energy isomer 9a is generated by capping the isomer 8a with one Si atom. This structure coincides with that for $AgSi_9$ obtained by Chuang et al.[53] The isomers 9b and 9c have a similar structure in which the Rb atom occupies different sites. The isomer 9d resembles the ground state structure of Si_{10}, which is 0.81 eV higher in energy than 9a isomer. For $RbSi_{10}$, the ground state isomer 10a is obtained by substituting the Rb impurity for one Si atom in the lowest-energy Si_{11} cluster. The isomers 10b and 10c are two tricapped tetragonal antiprism structures, in which the Rb atom locates in different sites. The isomer 10d, a Si-centered pentagonal prism structure, is 0.91 eV higher in energy than 10a. With regard to $RbSi_{11}$ cluster, we found that hexacapped prism isomer 11a is the lowest-energy structure, which can be viewed as the top Si atom in the ground state Si_{12} being substituted by one Rb atom. The isomer 11b, a bicapped pentagonal antiprism with one Rb atom on the vertex, is 0.35 eV higher in energy than 11a. This geometry is found as the low-lying YSi_{11} cluster in the article by Yang et al.[54] The isomer 11c is similar to the geometry of isomer 11a. However, the energy of 11c is higher than that of 11a by 0.67 eV. The isomers 11d and 11e are both the 4-4-4 layer structures, which are higher than 11a by 0.79 and 0.82 eV, respectively. When the number of Si atom is up to 12, five low energy isomers are found. The isomers 12a and 12c, which appear a structure similar to the lowest-energy configuration of Si_{13} cluster, are more stable than other isomers. The latter is higher in energy than the former by 0.53 eV. The other cubic isomers 12b, 12d, and 12e are energetically higher than that of 12a by 0.09, 0.86, and 1.13 eV, respectively.

From the above analysis on the structures of $RbSi_n$ clusters, it is obviously found that the most of the lowest-energy structures are similar with the ground state structures for the pure silicon clusters, which implies that the doped Rb atom faintly influence the geometries of the ground state Si_n clusters. This grow pattern is similar with the other alkali metals, such as Li, Na, and K, doped Si_n clusters, in which these clusters keep the Si_n framework unchanged.[33–35] During the search for the most stable isomers of the $RbSi_n$ clusters, the Rb-encapsulated into the Si cage structures are not found.

Relative stabilities of $RbSi_n$ ($n = 1$–12) clusters

To analyze the relative stabilities of $RbSi_n$ ($1 \leq n \leq 12$) clusters, the averaged binding energy $E_b(n)$, fragmentation energy $E_f(n)$, and second-order energy difference $\Delta_2E(n)$ are calculated using the following formulas[55,56]:

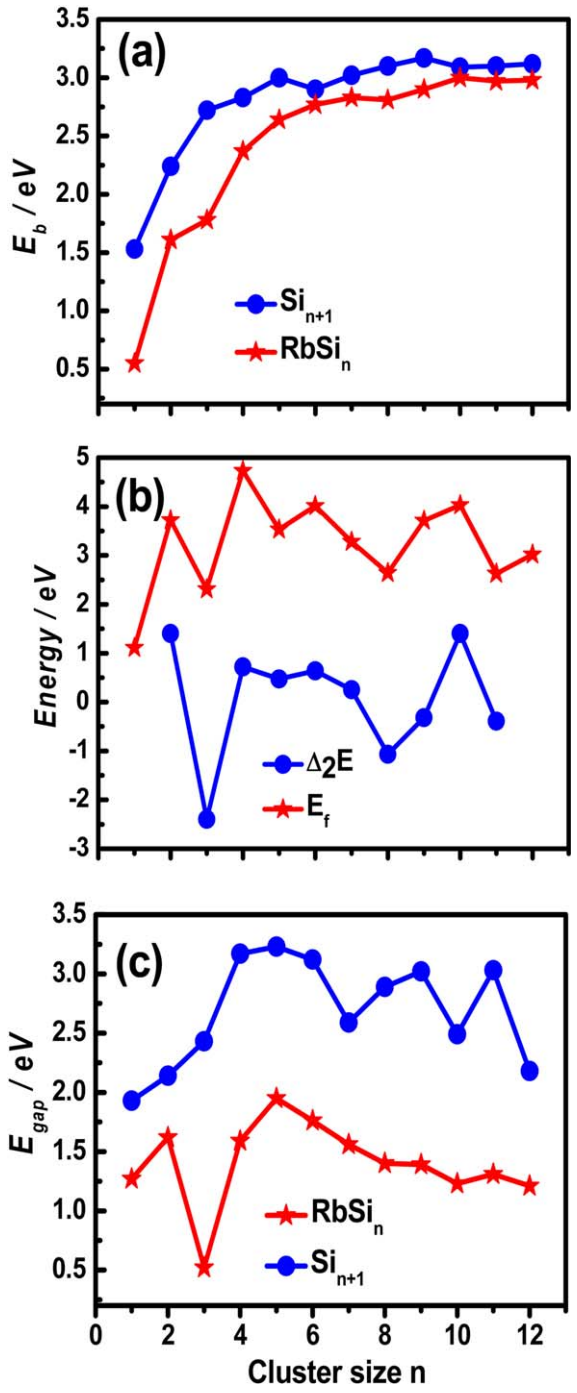

Figure 2. Size dependence of the averaged binding energy $E_b(n)$, fragmentation energy $E_f(n)$, second-order energy difference $\Delta_2E(n)$, and HOMO-LUMO energy gaps E_{gap} of the lowest-energy structures for Si_{n+1} and $RbSi_n$ clusters.

$$E_b(n)=[nE_k(Si)+E_k(Rb)-E_k(RbSi_n)]/(n+1) \quad (1)$$

$$E_f(n)=E_k(RbSi_{n-1})+E_k(Si)-E_k(RbSi_n) \quad (2)$$

$$\Delta_2E(n)=E_k(RbSi_{n+1})+E_k(RbSi_{n-1})-2E_k(RbSi_n) \quad (3)$$

where E_k(Rb) and E_k(Si) are the single atom energies for Rb and Si atom, and $E_k(RbSi_n)$, $E_k(RbSi_{n-1})$, and $E_k(RbSi_{n+1})$ are the total energies for the most stable $RbSi_n$, $RbSi_{n-1}$, and $RbSi_{n+1}$ clusters, respectively.

The $E_b(n)$, $E_f(n)$, and $\Delta_2E(n)$ values of the lowest-energy $RbSi_n$ clusters at the B3LYP/GENECP level are listed in Table 2 and shown as curves in Figure 2. From the Figure 2a, one can see that the $E_b(n)$ quickly increase as the cluster size of the $RbSi_n$ and Si_{n+1} clusters grows, where the $E_b(n)$ of $RbSi_n$ clusters are much smaller than those of pure Si_{n+1} clusters for $n \leq 5$. For $n = 6$–12, $E_b(n)$ of $RbSi_n$ and Si_{n+1} clusters slowly increase as the cluster size grows, with $E_b(n)$ of $RbSi_n$ clusters slightly smaller than that of Si_{n+1}. In other words, the doping of Rb atom decreases the chemical stability of Si_n clusters. This behavior of $Rb@Si_n$ clusters is similar to those of $CuSi_n$, $AgSi_n$, and Cu_2Si_n[37,53,55] clusters.

The second-order energy difference $\Delta_2E(n)$ and fragmentation energy $E_f(n)$ are two sensitive parameters that reflect the relative stabilities of clusters. As shown in Figure 2b, the $\Delta_2E(n)$ and $E_f(n)$ of $RbSi_n$ have the similar change tendency. For $\Delta_2E(n)$, four local prominent maxima are found at $n = 2$, 4, 6, and 10, implying that the $RbSi_2$, $RbSi_4$, $RbSi_6$, and $RbSi_{10}$ clusters have higher stability than their vicinal clusters. In addition, it shows odd-even oscillations except $n = 7$ and 8. When $n = 1$–6 and 9–12, even n give higher stability while odd n give lower stability. Specially, the $RbSi_2$ cluster exhibits the largest $\Delta_2E(n)$ of 1.40 eV among the Rh_2Si_n clusters, which may be used as the building block for novel cluster-assembled materials. For $E_f(n)$, five local peaks appear at the size of $n = 2$, 4, 6, 10, and 12, signifying that these clusters are relatively more stable than the others, which are in line with the maxima presented in the $\Delta_2E(n)$.

Electronic properties of $RbSi_n$ ($n = 1$–12) clusters

For the electronic properties, the highest occupied molecular orbital-lowest unoccupied molecular orbital (HOMO-LUMO) energy gaps E_{gap}, Mulliken charge populations (MP), partial density of states (PDOS), and chemical hardness (η) are calculated. The HOMO-LUMO energy gap E_{gap} is an important parameter for examining the electronic structure in cluster. In general, the smaller of E_{gap}, the lower energy is required to motivate the electrons from valence band to conduction band, corresponding to higher chemical activity of electronic structure.[57]

The E_{gap} of the ground state geometry on the doped $RbSi_n$ and pure Si_{n+1} clusters against the cluster size are shown in Figure 2c. As present in Figure 2c, three local peaks appear at $n = 2$, 5, and 11 for $RbSi_n$ clusters, indicating the higher chemical stability of these clusters relative to their neighbors. Based on the previous theoretical analysis of $E_b(n)$, $\Delta_2E(n)$, and $E_f(n)$, it can be concluded that the magic numbers of Rb-doped Si_n cluster is $RbSi_2$, reflecting that the $RbSi_2$ is the most stable structures. Besides, the range of E_{gap} for $RbSi_n$ clusters is lower than the corresponding pure Si_n clusters, which hints the increase in the metallic characteristics of Rb-doped Si_n clusters. This phenomenon is consistent with the behavior of $E_b(n)$.

To investigate the internal charge transfer information, we have performed a detailed analysis of the Mulliken charge

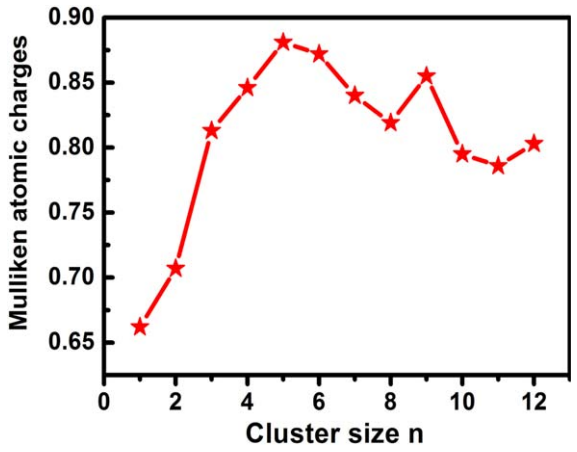

Figure 3. Size dependence of Mulliken charge population of Rb atom in the lowest-energy $RbSi_n$ ($n = 1$–12) cluster.

populations of the lowest-energy $RbSi_n$ clusters. The calculated results are listed in Table 2 and illustrated in Figure 3. As seen in the figure, the analysis of MP show that the ionic character of Rb—Si bond in these clusters. The Rb atom possess positive charges from 0.662 to 0.881 electrons, implying that charges always transfer from Rb atom to Si atoms, namely, Rb acts as the electron donor in all $RbSi_n$ clusters. This fact may be caused by the reason that the electronegativity of Rb (0.82) is much smaller than Si (1.90).[58] In addition, the size-dependence of charge transfer displays two kinds of trend. From RbSi to $RbSi_5$, the positive charge on Rb atom increases significantly. Then, from $RbSi_6$ to $RbSi_{12}$, the charge transfer of clusters decreases slowly except $RbSi_9$ and $RbSi_{12}$.

To further understand the effect of Rb atoms doping on electronic structure of Si_n clusters, the molecular orbital is calculated by examining the PDOS from the contribution of different orbital components (s and p) and electron density of the HOMO-LUMO states.[59,60] The calculated results of PDOS from the contribution of different orbital components (s and p) are listed in Table 2. Figure 4 gives the PDOS of some $RbSi_n$ ($n = 2$, 5, 6, and 11) clusters as representatives. From Table 2 and Figure 4, one can find some interesting characteristics: (i) the vertical dotted line indicates that the Fermi level is shifted to 0. (ii) The electronic states at the vicinity of Fermi level mainly originated from p state, and the contribution from s state is little. (iii) The change of PDOS (ρ_s and ρ_p) and total DOS (ρ_n) display oscillatory. For instance, the DOS of $RbSi_2$ cluster ρ_2 is lower than those (ρ_1

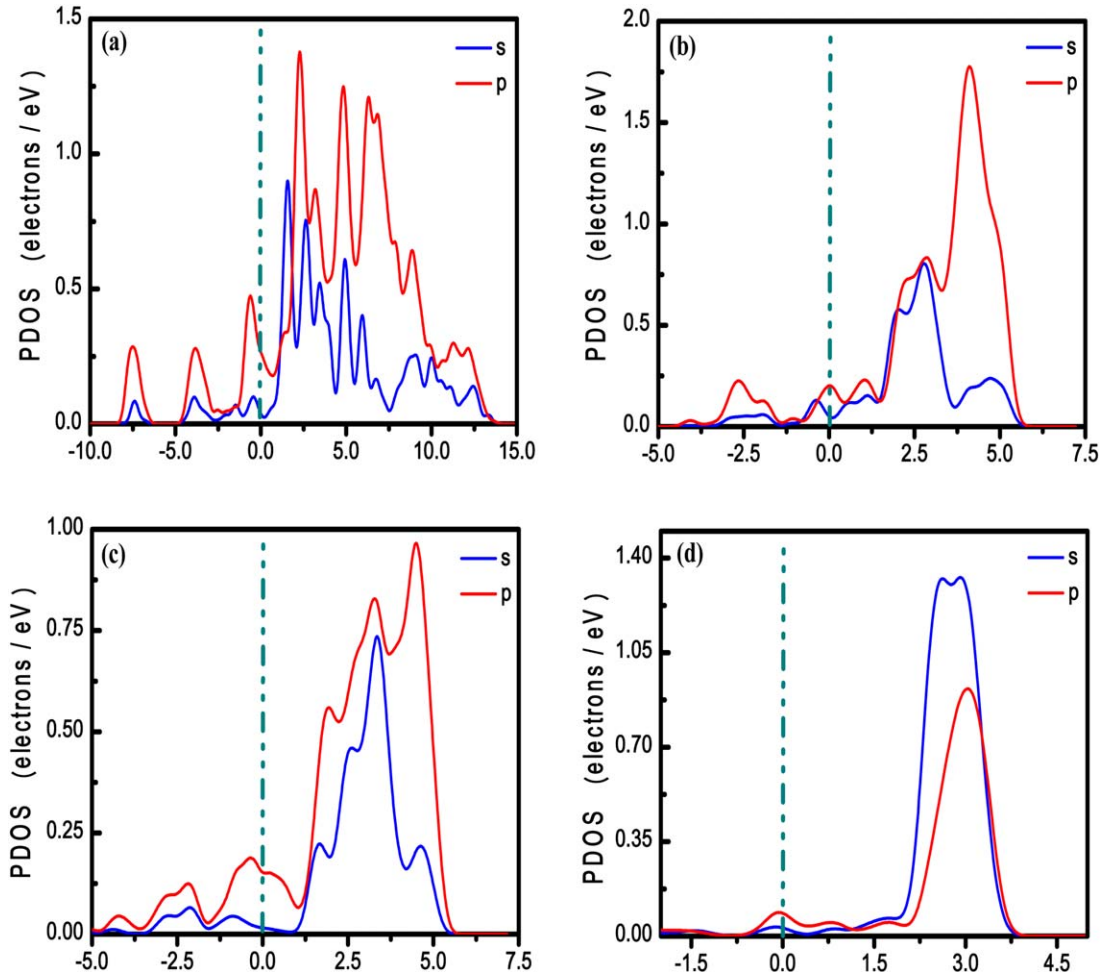

Figure 4. The PDOS of s, p orbital for (a) $RbSi_2$, (b) $RbSi_5$, (c) $RbSi_6$, and (d) $RbSi_{11}$.

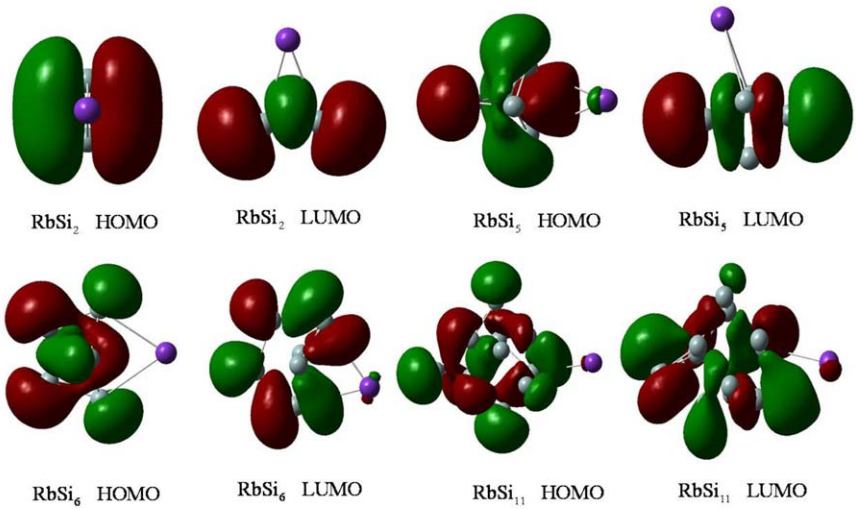

Figure 5. The HOMO and LUMO orbital of $RbSi_n$ ($n = 2$, 5, 6, and 11) cluster.

and ρ_3) of RbSi and $RbSi_3$ clusters whereas the DOS of $RbSi_8$ cluster ρ_8 is higher than those (ρ_7 and ρ_9) of $RbSi_7$ and $RbSi_9$ clusters. Similar case is also observed in the PDOS of $NiSi_n$[61] clusters.

The distribution of electron density of HOMO and LUMO states of some $RbSi_n$ clusters ($RbSi_2$, $RbSi_5$, $RbSi_6$, and $RbSi_{11}$) are plotted in Figure 5. From the figure, one can find that the most of HOMO and LUMO states are localized around Si atoms, while there are a few distributions around Rb atom.

Chemical hardness (η) is an important electronic parameter in many cases, which may be applied to determine the relative stability of molecules. On the basis of the principle of maximum hardness,[62] the η is defined as[63]

$$\eta = \mathrm{VIP} - \mathrm{VEA} \quad (4)$$

where VIP and VEA denote the vertical ionization potential and vertical electron affinity,[64,65] respectively. Therefore, the VIP, VEA, and η of the lowest-energy $RbSi_n$ and Si_{n+1} clusters are calculated and listed in Table 3. From the table, one can find some useful features: (i) the calculated VIP values of pure Si_{n+1} cluster have a small deviation compared with the experimental value of Si_{n+1} cluster. (ii) The theoretical VIP values for each size of $RbSi_n$ and Si_{n+1} clusters exhibit a sequence of $RbSi_n < Si_{n+1}$, so the metallic characteristics of pure Si_{n+1} frames have been enhanced by the impurity Rb atom. (iii) Three remarkable peaks of η appear at the size of 2, 5, and 11, which reflect that the $RbSi_{2,5,11}$ clusters are more harder than others. These results are in agreement with the Koopmans' theorem, in which a hard system has a large HOMO-LUMO gap and a soft system has a small HOMO-LUMO gap.[62] Specially, the $RbSi_2$ cluster has the largest η value of 5.59 eV (see Table 3), which implies that this cluster is extremely inert and may be useful to fabricate the cluster-assembled nanomaterials.[68] (iv) The η of the most stable $RbSi_n$ clusters are smaller than those of the corresponding Si_{n+1} clusters, which indicate that the doping of Rb atom can reduce chemical stability of pure Si_{n+1} clusters. This result is also in accord with the previous analysis based on $E_b(n)$ and E_{gap}.

Table 3. Chemical hardness (η), vertical electron affinity (VEA), and vertical ionization potential (VIP) of the lowest-energy Si_{n+1} and $RbSi_n$ ($n = 1$–12) clusters.

	$RbSi_n$			Si_{n+1}			
n	η (eV)	VEA (eV)	VIP (eV)	η (eV)	VEA (eV)	VIP (eV)	VIP [(eV) Exp.]
1	5.26	0.94	6.20	6.56	2.05	8.60	>8.49[66]
2	5.59	1.28	6.87	6.15	2.21	8.37	7.97–8.49[66]
3	3.35	2.09	5.44	6.03	2.11	8.14	7.97–8.49[66]
4	4.78	1.16	5.94	6.66	1.51	8.17	7.97–8.49[66]
5	5.18	1.37	6.55	6.67	1.36	8.02	~7.90[66]
6	4.72	1.14	5.86	4.95	2.96	7.91	7.46–7.87[66]
7	4.27	1.09	5.36	5.91	1.74	7.65	7.46–7.87[66]
8	4.14	1.50	5.65	6.07	1.82	7.89	~7.90[66]
9	4.00	1.64	5.64	5.79	2.08	7.87	7.46–7.87[66]
10	3.79	1.73	5.52	5.14	2.34	7.48	7.17–7.46[67]
11	3.91	1.79	5.70	4.58	2.68	7.26	7.17–7.46[67]
12	4.08	1.36	5.44	4.95	2.26	7.21	>8.49[67]

Conclusions

In this work, we have presented a systematic theoretical investigation on the geometries, stabilities, and electronic properties of $RbSi_n$ ($n = 1$–12) clusters using first-principles calculations at the B3LYP/GENECP level. The results are summarized as follows:

i. Compared with the pure Sin clusters, it is found that the ground state structures of $RbSi_n$ clusters can be obtained by substituting one surface Si atom of the lowest-energy structures of Si_n clusters with one Rb atom. In addition, the most stable isomers of RbSin clusters prefer 3D structures for n = 3–12.

ii. By analyzing the stabilities of RbSin clusters, it is found that the averaged binding energy $E_b(n)$ of these clusters are smaller than those of the corresponding pure Sin clusters. This indicates that the chemical activity of the silicon clusters can be enhanced by the impurity Rb atom. Moreover, the fragmentation energy $E_f(n)$, second-order energy difference $\Delta_2E(n)$ of RbSin clusters show a similar change tendency.

iii. The analysis results of HOMO-LUMO energy gaps Egap of RbSin clusters duplicate the conclusion drawn from the averaged binding energy $E_b(n)$. By combing the stabilities, one can conclude that the magic cluster is $RbSi_2$. The Mulliken population analysis show that the charges in $RbSi_n$ clusters always transfer from Rb atom to Si atoms.

iv. By analyzing the PDOS from the contribution of different orbital components (s and p), it is found that electronic state at the vicinity of Fermi level are mainly originated from p state. The most of HOMO and LUMO states are localized around Si atoms, while there are a few distributions around Rb atom.

Keywords: Rb-Si cluster • geometrical structures • electronic properties

How to cite this article: C.-G. Luo, C.-Z. He, H.-Y. Li, G.-Q. Li, S. Zhang, Liu, X.-Y. *Int. J. Quantum Chem.* **2014**, *115*, 50–58. DOI: 10.1002/qua.24796

[1] P. Claes, E. Janssens, V. T. Ngan, P. Gruene, J. T. Lyon, D. J. Harding, A. Fielicke, M. T. Nguyen, P. Lievens, *Phys. Rev. Lett.* **2011**, *107*, 173401.
[2] D. Palagin, M. Gramzow, K. Reuter, *J. Chem. Phys.* **2011**, *134*, 244705.
[3] S. Jaiswal, V. P. Babar, V. Kumar, *Phys. Rev. B* **2013**, *88*, 085412.
[4] M. B. Torres, E. M. Fernández, L. C. Balbás, *Int. J. Quantum Chem.* **2011**, *111*, 444.
[5] W. X. Ji, C. L. Luo, *Int. J. Quantum Chem.* **2012**, *112*, 2525.
[6] D. H. Ziella, M. C. Caputo, P. F. Provasi, *Int. J. Quantum Chem.* **2011**, *111*, 1680.
[7] G. S. Glander, M. B. Webb, *Surf. Sci.* **1989**, *222*, 64.
[8] R. Souda, W. Hayami, T. Aizawa, S. Otani, Y. Ishizawa, *Phys. Rev. Lett.* **1992**, *69*, 192.
[9] A. Namiki, S. Suzuki, H. Kato, Y. Babasaki, M. Tanaka, T. Nakamura, T. Suzaki, *J. Chem. Phys.* **1992**, *97*, 3781.
[10] R. Kishi, S. Iwata, A. Nakajima, K. Kaya, *J. Chem. Phys.* **1997**, *107*, 3056.
[11] D.Y. Zubarev, A. N. Alexandrova, A. I. Boldyrev, L. F. Cui, X. Li, L. S. Wang, *J. Chem. Phys.* **2006**, *124*, 124305.
[12] N. M. Tam, V. T. Ngan, J. de Haeck, S. Bhattacharyya, H. T. Le, E. Janssens, P. Lievens, M. T. Nguyen, *J. Chem. Phys.* **2012**, *136*, 024301.
[13] C. Sporea, F. Rabilloud, M. Aubert-Frécon, *J. Mol. Struct: Theochem* **2007**, *802*, 85.
[14] C. Sporea, F. Rabilloud, *J. Chem. Phys.* **2007**, *127*, 164306.
[15] P. Karamanis, R. Marchal, P. Carbonniére, C. Pouchan, *J. Chem. Phys.* **2011**, *135*, 044511.
[16] S. A. Blair, A. J. Thakkar, *J. Chem. Phys.* **2014**, *141*, 074306.
[17] E. Busman, *Z. Anorg. Allg. Chem.* **1961**, *313*, 90.
[18] C. Cros, M. Pouchard, P. Hagenmuller, *J. Solid-State Chem.* **1970**, *2*, 570.
[19] H. G. von Schnering, M. Somer, M. Kaupp, W. Carrillo-Cabrera, M. Baitinger, A. Schmeding, Y. Grin, *Angew. Chem.* **1998**, *110*, 2507.
[20] H. U. Borgstedt, C. Guminski, *Monatsh. Chem.* **2000**, *131*, 917.
[21] M. J. Frisch, G. W. Trucks, H. B. Schlegel, G. E. Scuseria, M. A. Robb, J. R. Cheeseman, J. A. Montgomery, Jr., T. Vreven, K. N. Kudin, J. C. Burant, J. M. Millam, S. S. Iyengar, J. Tomasi, V. Barone, B. Mennucci, M. Cossi, G. Scalmani, N. Rega, G. A. Petersson, H. Nakatsuji, M. Hada, M. Ehara, K. Toyota, R. Fukuda, J. Hasegawa, M. Ishida, T. Nakajima, Y. Honda, O. Kitao, H. Nakai, M. Klene, X. Li, J. E. Knox, H. P. Hratchian, J. B. Cross, V. Bakken, C. Adamo, J. Jaramillo, R. Gomperts, R. E. Stratmann, O. Yazyev, A. J. Austin, R. Cammi, C. Pomelli, J. Ochterski, P. Y. Ayala, K. Morokuma, G. A. Voth, P. Salvador, J. J. Dannenberg, V. G. Zakrzewski, S. Dapprich, A. D. Daniels, M. C. Strain, O. Farkas, D. K. Malick, A. D. Rabuck, K. Raghavachari, J. B. Foresman, J. V. Ortiz, Q. Cui, A. G. Baboul, S. Clifford, J. Cioslowski, B. B. Stefanov, G. Liu, A. Liashenko, P. Piskorz, I. Komaromi, R. L. Martin, D. J. Fox, T. Keith, M. A. Al-Laham, C. Y. Peng, A. Nanayakkara, M. Challacombe, P. M. W. Gill, B. G. Johnson, W. Chen, M. W. Wong, C. Gonzalez, J. A. Pople, Gaussian 09 Revision C.01; Gaussian, Inc.: Wallingford, CT, **2009**.
[22] A. D. Becke, *Phys. Rev. A* **1988**, *38*, 3098.
[23] C. Lee, W. Yang, R. G. Parr, *Phys. Rev. B* **1988**, *27*, 785.
[24] S. Zhang, W. Dai, H. Z. Liu, C. Lu, G. Q. Li, *J. Mol. Struct.* **2014**, *1075*, 220.
[25] Y. Liu, G. L. Li, A. M. Gao, H. Y. Chen, D. Finlow, Q. S. Li, *Eur. Phys. J. D.* **2011**, *64*, 27.
[26] C. Y. Xiao, F. Hagelberg, W. A. Lester, Jr., *Phys. Rev. B* **2002**, *66*, 075425.
[27] H. G. Xu, Z. G. Zhang, Y. Feng, J. Y. Yuan, Y. C. Zhao, W. J. Zheng, *Chem. Phys. Lett.* **2010**, *487*, 204.
[28] A. Fielicke, J. T. Lyon, M. Haertelt, G. Meijer, P. Claes, *J. Chem. Phys.* **2009**, *131*, 171105.
[29] M. Vogel, C. Kasigkeit, K. Hirsch, A. Langenberg, J. Rittmann, V. Zamudio-Bayer, A. Kulesza, R. Mitrić, T. Möller, B. V. Issendorff, J. T. Lau, *Phys. Rev. B* **2012**, *85*, 195454.
[30] J. T. Lyon, P. Gruene, A. Fielicke, G. Meijer, E. Janssens, P. Claes, P. Lievens, *J. Am. Chem. Soc.* **2009**, *131*, 1115.
[31] C. Pouchan, D. Bégue, D. Y. Zhang, *J. Chem. Phys.* **2004**, *121*, 4628.
[32] E. C. Honea, A. Ogura, C. A. Murray, K. Raghavachari, W. O. Sprenger, M. F. Jarrold, W. L. Brown, *Nature* **1993**, *366*, 42.
[33] J. C. Yang, L. H. Lin, Y. S. Zhang, A. F. Jalbout, *Theor. Chem. Acc.* **2008**, *121*, 83.
[34] L. H. Lin, J. C. Yang, H. M. Ning, D. S. Hao, H. W. Fan, *J. Mol. Struct: Theochem* **2008**, *851*, 197.
[35] D. S. Hao, J. R. Liu, W. G. Wu, J. C. Yang, *Theor. Chem. Acc.* **2009**, *124*, 431.
[36] Z. Y. Ren, F. Li, P. Guo, J. G. Han, *J. Mol. Struct: Theochem* **2005**, *718*, 165.
[37] D. Hossain, C. U. Pittman, Jr., S. R. Gwaltney, *Chem. Phys. Lett.* **2008**, *451*, 93.
[38] P. Guo, Z. Y. Ren, F. Wang, J. Bian, J. G. Han, G. H. Wang, *J. Chem. Phys.* **2004**, *121*, 12265.
[39] C. Amiot, *J. Chem. Phys.* **1990**, *93*, 8591.
[40] M. M. Kappes, E. Schumacher, *Surf. Sci.* **1985**, *156*, 1.
[41] K. P. Huber, G. Herzberg, Constants of Diatomic Molecules; Van Nostrand Reinhold: New York, **1979**.
[42] W. A. de Heer, W. D. Knight, M. Y. Chou, M. L. Cohen, *Solid State. Phys.* **1987**, *40*, 93.

[43] J. Lu, J. C. Yang, Y. L. Kang, H. M. Ning, *J. Mol. Model.* **2014**, *20*, 2114.
[44] C. Y. Xiao, J. Blundell, F. Hagelberg, W. A. Lester, Jr., *Int. J. Quantum Chem.* **2004**, *96*, 416.
[45] J. G. Han, Z. Y. Ren, B. Z. Lu, *J. Phys. Chem. A* **2004**, *108*, 5100.
[46] H. G. Xu, Z. G. Zhang, Y. Feng, J. Y. Yuan, Y. C. Zhao, W. J. Zheng, *Chem. Phys. Lett.* **2010**, *487*, 204.
[47] J. G. Han, C. Y. Xiao, F. Hagelberg, *Struct. Chem.* **2002**, *13*, 173.
[48] T. T. Cao, L. X. Zhao, X. J. Feng, Y. M. Lei, Y. H. Luo, *J. Mol. Struct: Theochem* **2009**, *895*, 148.
[49] J. Wang, J. G. Han, *J. Chem. Phys.* **2005**, *123*, 064306.
[50] B. X. Li, G. Y. Wang, W. F. Ding, X. J. Ren, J. Z. Ye, *Physica B* **2009**, *404*, 1679.
[51] S. Nigam, C. Majumder, S. K. kulshreshtha, *J. Chem. Phys.* **2006**, *125*, 074303.
[52] V. T. Ngan, E. Janssens, P. Claes, J. T. Lyon, A. Fielicke, M. T. Nguyen, P. Lievens, *Chem. Eur. J.* **2012**, *18*, 15788.
[53] F. C. Chuang, Y. Y. Hsieh, C. C. Hsu, M. A. Albao, *J. Chem. Phys.* **2007**, *127*, 144313.
[54] A. P. Yang, Z. Y. Ren, P. Guo, G. H. Wang, *J. Mol. Struct: Theochem* **2008**, *856*, 88.
[55] P. Shao, X. Y. Kuang, L. P. Ding, M. M. Zhong, Z. H. Wang, *Physica B* **2012**, *407*, 4379.
[56] H. Q. Wang, H. F. Li, J. X. Wang, X. Y. Kuang, *J. Mol. Model.* **2012**, *18*, 2993.
[57] X. J. Kuang, X. Q. Wang, G. B. Liu, *Eur. Phys. J. D* **2011**, *63*, 111.
[58] G. D. Zhou, L. Y. Duan, Structural Chemistry Basis; Peking University press: Beijing, **2002**.
[59] J. R. Li, G. H. Wang, C. H. Yao, Y. W. Mu, J. G. Wan, M. Han, *J. Chem. Phys.* **2009**, *130*, 164514.
[60] Y. F. Ouyang, P. Wang, P. Xiang, H. M. Chen, Y. Du, *Comput. Theor. Chem.* **2012**, *984*, 68.
[61] L. J. Li, C. H. Yao, Y. W. Mu, J. G. Wan, M. Han, *J. Mol. Struct: Theochem.* **2009**, *916*, 139.
[62] R. G. Pearson, Chemical Hardness: Applications from Molecules to Solids; Wiley-VCH: Weinheim, **1997**.
[63] D. Bandyopadhyay, *J. Mol. Model.* **2012**, *18*, 3887.
[64] Y. F. Li, X. Y. Kuang, A. J. Mao, Y. Li, Y. R. Zhao, *J. Mol. Model.* **2012**, *18*, 329.
[65] Y. R. Zhao, X. Y. Kuang, B. B. Zheng, S. J. Wang, Y. F. Li, *J. Mol. Model.* **2012**, *18*, 275.
[66] W. A. de Heer, W. D. Knight, M. Y. Chou, M. L. Cohen, *Solid State. Phys.* **1987**, *40*, 93.
[67] K. Fuke, K. Tsukamoto, F. Misaizu, M. Sanekata, *J. Chem. Phys.* **1993**, *99*, 7807.
[68] P. J. Bruna, S. D. Peyerimhoff, R. J. Buenker, *J. Chem. Phys.* **1980**, *72*, 5437.

Received: 18 July 2014
Revised: 31 August 2014
Accepted: 10 September 2014
Published online 25 September 2014